Journal of Multiscale Modelling
Vol. 1, No. 1 (2009) 177–196

ICP Imperial College Press
www.icpress.co.uk

MULTISCALE GENERATION OF TURBULENCE

S. LAIZET and J. C. VASSILICOS

Turbulence, Mixing and Flow Control Group, Department of Aeronautics, and Institute for Mathematical Sciences, Imperial College London, London, SW7 2BY, UK

This paper presents a brief but general introduction to the physics and engineering of fractals, followed by a brief introduction to fluid turbulence generated by multiscale flow actuation. Numerical computations of such turbulent flows are now beginning to be possible because of the immersed boundary method (IBM) and terascale parallel high performance computing capabilities. The first-ever direct numerical simulation (DNS) results of turbulence generated by fractal grids are detailed and compared with recent wind tunnel measurements.

Keywords: Turbulence; fractals; non-linear physics; fluid mechanics; multiscale flow control; multiscale dynamics; direct numerical simulations; immersed boundary method.

1. A Multilevel Introduction

Nineteenth century mathematics stumbled upon exciting and intriguing new concepts such as nowhere-differentiable continuous functions, Cantor sets and Koch curves, and various related fundamental questions, such as how to define the age-old concept of dimension. Caratheodory[1] gave a definition of dimension which was subsequently generalised by Hausdorff[2] to non-integer dimensions. Thus, the concept of geometrical forms, sets of points and functions with non-integer fractal dimensions was born, Cantor sets and Koch curves being examples of such sets and forms. Work on these extraneous and abstract mathematical objects carried on quietly in some departments of pure mathematics around the world, such as in the University of Cambridge, where A. S. Besicovitch, followed by S. J. Taylor (Besicovitch's PhD student), kept this esoteric activity alive from the 1930s all the way to the 1980s and beyond (see, for example, Falconer's book on fractal geometry[3]). In the 1970s Mandelbrot[4,5] successfully forced the realisation into the minds of scientists of all denominations that shapes and forms with non-integer dimensions are not exceptional but in fact pervasive in nature, and coined the word "fractal" to describe such shapes. Suddenly, these fractal shapes and geometries were not the preserve of pure mathematicians any longer and a frenzy of activity followed by a wide variety of scientists who set out to measure the fractal dimensions of nearly everything under the sun and beyond: clouds, trees, birdsong, geological sites, geomorphology and coastlines, stock market fluctuations, fluid turbulence, polymers, fractures, the

sky distribution of stars...even Chinese landscape paintings. This fractal-spotting activity gave rise to such an enormous number of publications and conferences that the eventual emptiness of the endeavour became embarrassingly apparent to those prepared to confront it. In a paper published in 1986 with the title "Fractals: Where Is the Physics?", Kadanoff[6] wrote, referring to this fractal-spotting frenzy, that "much of the work on fractals seems somewhat superficial and even slightly pointless" and that "the physics of fractals is, in many ways, a subject waiting to be born". (The term "fractal" in these statements can be understood in the broadest sense of a geometrical structure which cannot be described in any non-multiscale way. This is also the sense in which the term "fractal" is used in this paper.)

The point had nevertheless been made that fractal shapes and forms can fit an effectively infinite length within a finite area and an effectively infinite area within a finite volume. Human lungs are a stunning example of this fact: they are fractal and, as a result, can cover an entire tennis court if unfolded! It seems that nature uses fractal shapes to maximise contact within finite confines: trees rely on their fractal shape to maximise photosynthesis and lungs rely on their fractal shape to maximise provision of oxygen to the bloodstream. These fractal shapes and the non-integer fractal dimensions which characterise them result from their multiscale geometrical structure.

These were all good points, but it was necessary by the mid-1980s to start extracting their physical and mechanical consequences and start developing what Kadanoff had called "the physics of fractals". The development of the physics of fractals started slowly in the mid-1980s with works by Berry,[7] for example, who showed how the power of waves diffracted off fractal surfaces and the diffusion of fractal aerosols are dramatically altered by fractal boundaries. In the 1990s, Sapoval *et al.*,[8] started depositing soap bubbles on fractal boundaries and directing sound waves on these bubbles. Their laboratory experiments (which carried on into this decade) revealed that fractal boundaries effectively soak up vibrational energy so that some vibrations are dumped extremely quickly, resulting in small regions of the bubble vibrating noticeably whilst the rest hardly moves. Lapidus *et al.*,[9] studied the harmonics of the vibrating fractal drum both analytically and numerically, with conclusions that indicate that the fractal dimension of the drum can effectively be "heard". Fleckinger *et al.*,[10] and van den Berg[11] solved the heat equation for the temperature field in open regions possessing a fractal boundary held at constant temperature. They were able to show that the rate at which heat is lost at initial times increases with the fractal dimension of the boundary.

Without being exhaustive, this list of works more or less summarises the initial directions of research in this emerging field of study, the physics of fractals, over the past 20 years. The defining characteristic of these initial research directions is their concern with linear dynamics (e.g., wave and heat equations) constrained by fractal boundary and initial conditions. The issues are about how the multiscale nature of boundary/initial conditions permeates into the linear dynamics which would not have had multiscale characteristics otherwise.

Engineering with fractals started rather timidly in the mid-1990s and remains, to this day, hardly visible. Fractal Antenna Inc (founded 1995) sell fractal antennae which have superior multiband performance and are typically 2–4 times smaller than traditional aerials. Amalgamated Research Inc (mid-1990s to this day) sell fractal fluid injectors for gases and liquids and develop fractal solutions for industrial scale chromatography and uniform air circulation in sugar silos. In 2005, the Fraunhofer Institute for Solar Energy Systems advertised fractal hydraulic structures for solar absorbers and other heat exchangers. But that is more or less it, and the market penetration has been extremely limited. It may be a surprise that in spite of their clear advantages, fractal antennae, for example, do not grace the rooftops of most major cities. The long march from pure mathematics to applied mathematics to physics and mechanics and eventually to engineering is only half the way, in those rare cases of commercially successful innovation, to prototyping, commercialising and eventually creating a new business venture and/or successful commercial product. Innovations have to overcome many so-called adoption hurdles (strong resistance from various stakeholders and frozen inertia and conservatism at the sight of the unknown)[12] and successful innovators need to have the ability to overcome these hurdles. Edison famously said that his work was 1% inspiration and 99% perspiration; his success would obviously not have been possible without his inventions but it was his unique and celebrated abilities in overcoming adoption hurdles which contributed 99% of the acumen necessary for his success, the remaining 1% being attributable to his necessary but sadly secondary genius as an inventor.

Now, near the end of the first decade of the 21st century, there remain two important challenges in this broad line of activity. Firstly, whilst some progress has now been made in the linear physics of fractals, the *non-linear physics of fractals* still remains "a subject waiting to be born", to use Kadanoff's turn of phrase. Secondly, there is a lot of potential *engineering applications of fractals* that have never been tried. A good place to start addressing both these challenges is fluid mechanics in the high Reynolds number turbulence regime, which is the regime most often encountered in nature and industry.

Studies of low Reynolds number and non-turbulent hydrodynamic properties of fractals[13,14] have been made as part of the developments in the linear physics and mechanics of fractals over the past 25 years or so. But conclusive studies of the full non-linear behaviour of turbulent flows generated by or interacting with fractal boundaries have only started to appear very recently,[15,16] following the rather clumsy but first-ever such attempt by Queiros-Conde and Vassilicos[17] in 2001.

The non-linear dynamics of the Navier–Stokes equations for incompressible flow spontaneously generate multiscale excitations characterised by multiscale intermittency and multiscale order/disorder and coherence. In the case of the atmospheric boundary layer, for example, excited turbulent eddies range from the millimetre to the kilometre so that the multiscale range of excitations spans six decades. It is

currently impossible to resolve and simulate the entirety of this very wide range of eddy scales. This hurdle results single-handedly from the non-linear mechanics of fluid flow — not even from the coexistence of various physical mechanisms acting at different scales and interacting with each other, as is the case in a multitude of multiscale problems. This extra multiscale complication does often present itself in many fluid flow problems, such as in turbulent flames and chemical reactors where the combustion and chemistry introduce their own scales and non-linear mechanisms. The example of polymer-laden turbulent flows for turbulent drag reduction purposes may be particularly instructive, because it clearly distinguishes between length scales and time scales and highlights their relative importance: the polymer dynamics are characterised by length scales (molecule lengths) ranging between 10^{-12} m and 10^{-9} m, whereas the smallest turbulent eddy may be as small as 10^{-7} m. However, the polymer motions (local bond dynamics, Rouse dynamics, stretch-coil relaxation) are characterised by time scales ranging between 10^{-12} s and 10^{-2} s and the turbulent eddy time scales range from 10^{-5} s to 10^{2} s (and even above in the atmosphere). Whereas there is no overlap in length scales, there is a clear overlap in the time scales of the polymer and the turbulence dynamics. Multiscale approaches to polymer drag reduction must therefore take this observation into account[18] when attempting to simulate the observed drag reduction brought about by polymer stretch mechanisms and explain why drag reduction, which is a large-scale phenomenon, can be caused by polymer dynamics, which are small-scale.

In fact, polymers have complex multiscale dynamics of their own, as well as multiscale fractal geometrical structures of their own.[18,19] The full multiscale problem of polymer-laden turbulent flows would therefore comprise two sub-problems, both of a multiscale nature but each of a single physical nature. Each of these problems can be quite daunting in itself, and the turbulence problem without polymers, in particular, is widely regarded as one of the greatest unsolved problems in classical mechanics. In this paper we address the multiscale dynamics generated by the high Reynolds number physics of incompressible fluid flow non-linearities without extra multiphysics effects, as this problem is a milestone for progress in various other multiscale and multiphysics fluid flow problems. For example, understanding and modelling the multiscale and multiphysics problem of turbulent drag reduction by polymer additives cannot be expected without an understanding of the multiscale energy and momentum transfers in a turbulent flow without polymers.

However, the main difference between this paper and other works on turbulent flows is that we consider turbulence generated by multiscale stirrers, i.e., multiscale non-linear flows generated by multiscale turbulence generators. As such, this paper contributes both to the emerging *non-linear physics of fractals* and to its sub-topic *flow–fractal interactions*, which may come to be seen as a pillar of future multiscale modelling for that particular range of flow applications involving complex multiscale boundaries such as mountain and ocean floor topographies, plant canopies,[20] trees,[21] coral reefs[22] and respiratory systems.[23] The necessity to investigate turbulent fluid flows over and through such multiscale structures arises

from urgently pressing issues such as flood management, pollutant dispersal, atmosphere/biosphere interactions, and atmosphere–ocean interactions via the fractal whitecap, all crucial for Met Office, environmental and climate predictions and subsequent governmental and intergovernmental decisions concerning crisis management of accidents and natural disasters, the environment and climate change.

The necessity to investigate turbulent flows generated and/or interacting with multiscale fractal structures also arises from new prospects for engineering applications of flow–fractal interactions. For example, it was recently demonstrated that fractal grids can be used as energy-efficient stirring elements for inline static mixers and that, even without optimisation, they compare favourably with commercially available state-of-the-art stirring elements.[24] There are also countless other possibilities, including fractal dynamic mixers, fractal ventilation, fractal combustors, fractal burners, fractal airbrakes, fractal flaps, etc. These can all be seen as part and parcel of a new flow engineering approach called *multiscale flow control*,[15,25,26] which may be either passive or active, and, if active, either with or without feedback. Two patents concerning fluid flow modification for applications such as the ones just mentioned have already been filed by Imperial Innovations.

To address these necessities, we present in this paper the first-ever direct numerical simulation (DNS) of turbulent flows generated by fractal objects (with the exception of a few computer-generated graphics presented at the Gallery of Fluid Motion at the APS 60th Annual Meeting of the Division of Fluid Mechanics[27] and in Physica Scripta[58]). The fractal objects considered here are the fractal grids used in recent wind tunnel experiments[15,16] on turbulence generated by fractal grids. The results obtained from these recent wind tunnel experiments strongly suggest that all currently available turbulence-modelling approaches, including RANS (Reynolds averaged Navier–Stokes) and LES (large eddy simulation), cannot be used to simulate fractal-generated turbulence as the properties of these flows differ from all known turbulent flows in profound ways.[15,16] Most notably, the turbulent kinetic energy dissipation rate per unit mass in homogeneous isotropic turbulence generated by some fractal grids in the wind tunnel is not independent of Reynolds number, as it is assumed to be in Kolmogorov phenomenology,[28] in LES subgrid modelling and in one-point closures[29] such as $k - \epsilon$.

Nevertheless, a modelling approach and numerical technique for simulating turbulence interacting with idealised fractal trees was proposed last year.[30] It is called renormalised numerical simulation (RNS) and takes advantage of an assumed scale invariance in some flow properties to model subgrid scales. These simulations allow only calculations of drag on fractal bodies and not of turbulence generated by them. Furthermore, the strong assumptions concerning the drag's dependence on the multiscale fractal iterations which they rely on are totally untested. It is therefore imperative to develop DNSs of multiscale-generated turbulence and use the recent experimental results to validate them so that the DNSs and laboratory experiments combined may eventually serve as a foundation for multiscale modelling approaches such as RNS.

The remainder of this paper is structured as follows. Section 2 is a brief overview of recently emerging laboratory studies of turbulence generated by fractal grids. In Sec. 3 we very briefly introduce the immersed boundary method (IBM), and in Sec. 4 we report how this method may be combined with the well-known fractional step method. In Sec. 5, we present the first-ever DNSs of a turbulence generated by a fractal grid. We conclude in Sec. 6.

2. Turbulence Generated by Multiscale Grids

Turbulence is of enormous importance in the environment, meteorology and oceanography, and also in many industries where fluid flow is involved, such as the chemical, mixing, car, aerospace and naval industries. For example, the cost of pumping oil through pipelines is directly proportional to the frictional losses caused by turbulence. Understanding turbulence can lead to flow control schemes for reducing skin friction drag. At US$100 per barrel (a conservative estimate nowadays), 10% such reduction would save worldwide ocean shipping (which consumes about 2.1 billion barrels of oil per year) about US$21 billion per year, not to mention the consequent impressive reductions of pollutants in ship emissions. Similar projections can be made for airline industries, which consume about 2 billion barrels of jet fuel per year. Improvements in turbulence management can also be brought to combustion engines and mixing devices, thus leading to further energy gains and emission reductions.

Over the past 60 years or so, the efforts in turbulence have been mostly in *ad hoc* modelling of specific turbulent flows and the progress has been limited. A fundamental understanding of turbulence dynamics is needed, and for this a well-designed and well-targeted experiment is required where these turbulence dynamics can be set out of joint so as to give us clues for understanding them.

This is what has been recently achieved at Imperial College London, where the first wind tunnel experiments to contribute unambiguous results on turbulence generated by fractal grids have been conducted.[15,16] These authors used hot wire anemometry and investigated the scaling and decay of turbulence generated downstream of 21 different two-dimensional fractal grids pertaining to three different families: fractal cross, fractal square and fractal I grids (see Fig. 1). Their wind tunnel experiments have shown that the turbulence intensity of fluid turbulence generated by planar fractal grids depends on the grid's fractal parameters as well as on the pressure drop across it.[15] It is therefore possible to independently set the levels of turbulence intensity and pressure drop. Fractal grids can be designed to generate high turbulence intensities with low pressure drops, in which case one has energy-efficient mixers, but can also be designed to have low turbulence intensities with high pressure drops, in which case one may have relatively silent airbrakes.

One of the most interesting results of these experiments is that, for a particular class of fractal grids, i.e., the fractal square grids, two regions exist downstream of the grid: a turbulence production region followed by a turbulence dissipation

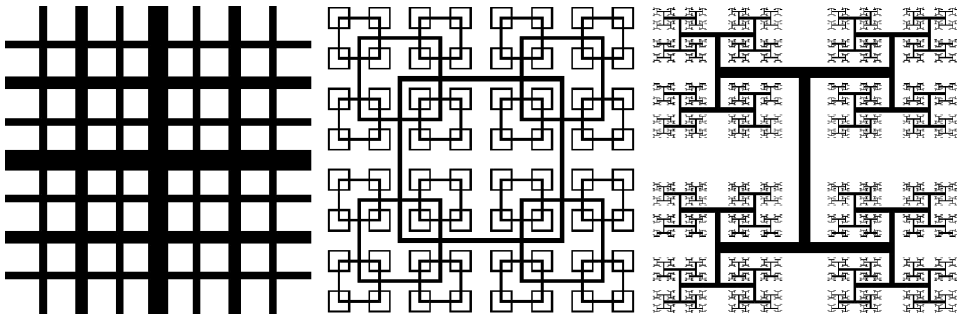

Fig. 1. Scaled diagrams of a fractal cross grid (left), a fractal square grid (middle) and a fractal I grid (right).

region where the turbulence is statistically homogeneous and isotropic.[15,16] Other families of fractal grids behave differently on the centreline and do not exhibit a progressive turbulence build-up downstream of the grid on the centreline. The various velocity profiles, correlations, spectra and coherence spectra in the free decay region indicate that the turbulence is homogeneous and isotropic to a satisfactory approximation there. Yet, remarkably, the integral and Taylor length scales remain constant during decay downstream of fractal square grids (as opposed to classical mesh grids, where they markedly increase, and fractal cross and I grids on the centreline, where they also increase). The most recent experiments on turbulence generated by fractal square grids[16] indicate that the kinetic energy dissipation scales as ${R_\lambda}^{-1}$ (R_λ is the Reynolds number based on Taylor's micro-scale) over the range from O(100) to O(1000) and reaches values that are an order of magnitude smaller than in any approximately isotropic turbulence experiment to date. However, the flow is fully turbulent with an energy spectrum that has a clear $-5/3$ range. There is also intriguing evidence that the interscale energy transfers are severely modified in fractal-generated turbulence even very far downstream.[31] These properties are completely different from those of any turbulent flow studied to date and run counter to the classical views on turbulence stemming from Taylor[32] and Kolmogorov,[28] who set the foundations of modern turbulence research. In particular, all modelling approaches and all theories of turbulence assume that the kinetic energy dissipation rate is independent of R_λ. These unprecedented results indicate that the turbulence in flows past fractal objects cannot be modelled using any of the existing and/or conventional approaches.

Moreover, fractal grids can be designed as stirring elements for inline static mixers and, as shown by recent proof-of-concept experiments,[24] they compare favourably with commercially available state-of-the-art stirring elements. This has been achieved without time for optimisation and adaptation. Hence, possibilities for improvement are vast, with the potential to set new industrial mixing standards, at least for some mixing applications.

The next steps which are now unavoidable for progress in this new field of research is to perform large DNSs and stereoscopic particle image velocimetry (SPIV) measurements in order to explain and extend the recent wind tunnel anemometry measurements described above. Although these measurements have provided invaluable time-resolved information on the unique properties of our flows, understanding the spatial structure of these flows will be necessary for understanding the origins of these properties. In this paper we address the DNS need but leave the SPIV need for future studies.

Fundamental scientific questions which require more elaborate experimental measurement techniques and the exceptionally large DNS proposed here include the following: what causes the protracted turbulence production region in the lee of fractal square grids? Is the reason related, and if so how, to the expectation that small turbulence eddies resulting from the many but small fractal iterations are advected and breakup into a turbulence cascade nearer the grid than larger turbulence eddies which result from the less numerous but larger fractal iterations? What does this imply for the spectral development of the turbulence as it is advected away from the grid? Why does this multiscale turbulence generation lead, in the far-downstream decay region where this generation has ceased, to what appear to be major modifications of interscale energy transfers and a depletion or capping of vorticity and strain generation such that it does not amplify with increasing Reynolds number? Are direct "long-range" couplings between the largest and the smallest turbulence eddies involved in this process? What kind of phase couplings does the fractal generation of the turbulence impose for that turbulence to remain so non-classical for such a long distance downstream from the grid?[15,16,31] How are the alignments/misalignments[33] of the vorticity and strain rate tensor in fractal-generated turbulence? These questions matter as they directly relate to interscale energy transfer, and as the energy spectrum of this non-classical turbulence appears to have a well-defined $-5/3$ power law range seemingly regardless of these couplings and alignments. Is the turbulence generated by different types of fractal grids really different, or is it similar in appropriately chosen parts of the flow? Important related questions are concerned with the decay rate of scalar fluctuations in fractal-generated turbulence and the evolution of the scalar integral and Taylor length scales during decay. How are the alignments or misalignments between scalar gradients and vorticity/strain rates affected by the fractal generation of the turbulence? What are the implications for energy-efficient mixing and combustion and for flame stability, ignition and extinction? Which fractal grids and with what fractal grid parameters may give the best mixing and combustion efficiency, i.e., what is the best possible fractal design for energy-efficient (i.e., a low-pressure drop across the grid) generation of high turbulence intensities and homogeneous flows as required for efficient mixing?

In the following sections, we present the DNS code that we use to compute turbulent flow fields generated by multiscale/fractal grids and the results obtained with our DNS.

3. DNS of Turbulence Generated by Multiscale Grids Based on the Immersed Boundary Method

The most faithful simulations of turbulence involve solving the Navier–Stokes equations without averaging, filtering, modelling or approximating other than numerical discretisations. In such simulations all the motions are resolved at all scales and the computed flow field is equivalent to a particular single realisation. If run over a long enough time, the statistics of this realisation may be expected to coincide with the statistics over many realisations. This approach, DNS, is applied here to turbulence generated by multiscale/fractal grids such as those of Fig. 1.

The multiscale nature of our fractal grids gives them a complicated geometrical shape where it is difficult to satisfy flow boundary conditions whilst at the same time solving the Navier–Stokes equation for an incompressible flow with a high-order numerical scheme.[34] Despite the continual progress of computers, that kind of turbulent flow with complex geometries remains a difficult task. Indeed, a compromise must be found in order to correctly describe the physics of the flow for a reasonable computational cost. One of the most popular approaches is to generate sophisticated meshes following the solid geometry. However, such simulations remain expensive for a relatively small numerical accuracy, due to the distortion of the mesh. An alternative strategy can be found with codes based on a Cartesian mesh combined with the immersed boundary method (IBM). We use here the generic term IBM introduced by Peskin,[35] where the idea was to consider the fluid–structure interaction problem involving blood flow in the human heart. The advantage offered by the IBM is its ability to take into account flexible boundaries and their dynamic shape changes whilst solving the Navier–Stokes equations on a Cartesian mesh. However, one does not need to be confronted with dynamic flow–structure interactions and elastic boundaries[36] for the IBM to be of use. A sub-class of IBM methods has been developed for simulating flows with complex embedded solid boundaries[37–39] which do not conform to the shape of the mesh. The reader interested in a broad review of the IBM can find one[40] published a few years ago in *Annual Reviews of Fluid Mechanics*. In this paper we focus on the IBM for solid, non-moving boundaries which acquire their complexity from their multiscale geometry.

Three types of the IBM can be distinguished: a feedback forcing introduced by Goldstein *et al.*,[41] which is based on an artificial term that can cancel the fluid in the body region through a damping oscillation process; an algebraic forcing by Arquis and Caltagirone,[42] which corresponds to the modelling of a porous medium, and the limit case of zero porosity leads to the modelling of a solid surface; and a direct forcing by Fadlum *et al.*,[39] where the boundary condition is ensured directly on the velocity using a forcing term at each time step of the time integration. Unfortunately, feedback and algebraic forcing have a common drawback related to their numerical stability properties. Indeed, both methods lead to a severe additional restriction on the time step to maintain very low residual velocities at the limit of

the body surface. In order to avoid this limitation, the use of a direct forcing is very attractive. This forcing is implemented as an additional term in the Navier–Stokes equation. This allows the use of a Cartesian mesh, which in turn allows the implementation of a high-order compact finite difference scheme.

4. Implementation of the Forcing Combined with a Fractional Step Method

To solve the incompressible Navier–Stokes equations, we use a numerical code (called "Incompact3d") based on sixth-order compact schemes for spatial discretisation and a second-order Adams–Bashforth scheme for time advancement. To treat the incompressibility condition, a fractional step method[43–47] requires one to solve a Poisson equation. This equation is fully solved in the spectral space, via the use of relevant 3D fast Fourier transforms. This allows us to consider all the combinations of free-slip, periodic or Dirichlet boundary conditions on the velocity field in the three spatial directions. In the calculations presented here, boundary conditions are only inflow/outflow in the direction x of the mean flow (velocity boundary conditions of the Dirichlet type) and periodic in the directions y and z. The pressure mesh is staggered from the velocity mesh to avoid spurious pressure oscillations. With the help of the concept of modified wave number, the divergence-free condition is ensured up to machine accuracy. An extra potential advantage which we do not make use of here is the possibility of introducing mesh stretching in one direction without losing the non-iterative nature of the Poisson solver.[48] It should be noted also that solving the Poisson equation in the spectral space has a cost limited to less than 15% of the overall computational expense. More details about the present code and its validation, especially the original treatment of the pressure in the spectral space, can be found in the papers of Laizet and Lamballais.[49,50]

The modelling of the fractal grids is performed by a forcing term following the procedure proposed by Parnaudeau *et al.*,[51] which ensures the no-slip boundary condition on the fractal grids. Note that our particular Cartesian mesh does, in fact, conform to the geometries of the fractal grids of Fig. 1 because they consist of right angles and are placed normal to the mean flow. *A priori*, the combination of a high-order scheme with an IBM can be problematic because of the discontinuity in velocity derivatives locally imposed by the artificial forcing term. However, even though the formal order of the solution is reduced as a result, the code has been demonstrated to be far more accurate with a sixth-order scheme than with a second-order scheme in both statistics and instantaneous field realisations.[49–54]

The governing equations are the forced incompressible Navier–Stokes equations

$$\frac{\partial \mathbf{u}}{\partial t} = -\nabla \mathbf{p} - \frac{\mathbf{1}}{\mathbf{2}} \left[\nabla(\mathbf{u} \otimes \mathbf{u}) + (\mathbf{u} \cdot \nabla)\mathbf{u}\right] + \nu \nabla^{\mathbf{2}} \mathbf{u} + \mathbf{f}\,, \tag{1}$$

$$\nabla \cdot \mathbf{u} = 0\,, \tag{2}$$

where $p(\mathbf{x}, t)$ is the pressure field (for a fluid with a constant density $\rho = 1$) and $\mathbf{u}(\mathbf{x}, t)$ the velocity field. More details about the exact expression of the forcing term

$\mathbf{f}$ will be given below. Note that the convective terms are written in skew-symmetric form. This specific form reduces aliasing errors while remaining energy-conserving for the type of spatial discretisation considered here. It is therefore the form used in our code.

In the framework of the fractional step method, several adjustments are necessary in order to eliminate the various couplings introduced by the implicit nature of the forcing used here. Indeed, the basic idea is to impose the forcing on the velocity at the end of each time step. For this reason, using a a second-order Adams–Bashforth scheme, a three-step advancement of the forced Navier–Stokes equations is required and can be expressed as

$$\frac{\mathbf{u}^* - \mathbf{u}^k}{\Delta t} = \frac{3}{2}\mathbf{F}^k - \frac{1}{2}\mathbf{F}^{k-1} - \nabla\tilde{\mathbf{p}}^k + \tilde{\mathbf{f}}^{k+1}\,, \tag{3}$$

$$\frac{\mathbf{u}^{**} - \mathbf{u}^*}{\Delta t} = \nabla\tilde{\mathbf{p}}^k\,, \tag{4}$$

$$\frac{\mathbf{u}^{k+1} - \mathbf{u}^{**}}{\Delta t} = -\nabla\tilde{\mathbf{p}}^{k+1}\,, \tag{5}$$

with

$$\mathbf{F}^k = -\frac{1}{2}\left[\nabla\left(\mathbf{u}^k \otimes \mathbf{u}^k\right) + (\mathbf{u}^k \cdot \nabla)\mathbf{u}^k\right] + \nu\nabla^2\mathbf{u}^k \tag{6}$$

and

$$\tilde{p}^{k+1} = \frac{1}{\Delta t}\int_{t_k}^{t_{k+1}} p dt\,, \quad \tilde{\mathbf{f}}^{k+1} = \frac{1}{\Delta t}\int_{t_k}^{t_{k+1}} \mathbf{f} dt\,. \tag{7}$$

In this writing, the pressure and forcing terms are used only through their time-averaged values on a given step Δt, which is indicated by the tilde in $\tilde{p}^{k+1}$ and $\tilde{\mathbf{f}}^{k+1}$.

In a classical fractional step method without forcing term, the incompressibility condition (2) can be verified at the end of each sub-time-step,

$$\nabla \cdot \mathbf{u}^{k+1} = 0\,, \tag{8}$$

through solving a Poisson equation,

$$\nabla \cdot \nabla\tilde{\mathbf{p}}^{k+1} = \frac{\nabla \cdot \mathbf{u}^{**}}{\Delta t}\,, \tag{9}$$

which provides the estimation of $\tilde{p}^{k+1}$ necessary for performing the correction (5). In a general IBM, the forcing term is defined such as to verify more or less rigorously the expected boundary condition at the wall of the body.[a] In the present study, we use a direct method and the forcing term in (3) is expressed as

$$\tilde{\mathbf{f}}^{k+1} = \varepsilon\left(-\frac{3}{2}\mathbf{F}^k + \frac{1}{2}\mathbf{F}^{k-1} + \nabla\tilde{\mathbf{p}}^k + \frac{\mathbf{u_0}^{k+1} - \mathbf{u}^k}{\Delta t}\right), \tag{10}$$

with $\varepsilon = 1$ in the body region and $\varepsilon = 0$ everywhere else. As for a conventional Dirichlet condition, the present definition of $\tilde{\mathbf{f}}^{k+1}$ allows the exact prescription of $\mathbf{u}^*$

[a]See Ref. 40 for a review of the diversity of techniques already successfully developed.

in the forcing region so that the final error on $\mathbf{u}^{k+1}$ is second-order in time, namely $\mathbf{u}^{k+1} = \mathbf{u_0}^{k+1} + O(\Delta t^2)$ when $\varepsilon = 1$. The target velocity $\mathbf{u_0}(\mathbf{x}, t)$ is calibrated in order to verify the no-slip condition at the wall of the body while ensuring the regularity of the velocity field across the immersed surface (see Ref. 51 for more details). Note that for the fractal grids, this target velocity $\mathbf{u_0}$ is zero, but as the target velocity is not necessarily divergence-free, Parnaudeau *et al.*,[51] have proposed solving a specific pressure equation,

$$\boldsymbol{\nabla} \cdot \boldsymbol{\nabla} \tilde{p}^{k+1} = \frac{\boldsymbol{\nabla} \cdot [(1-\varepsilon)\mathbf{u}^{**}]}{\Delta t}, \tag{11}$$

where the conventional Poisson equation (8) is recovered for $\varepsilon = 0$, whereas inside the body the condition $\varepsilon = 1$ yields the Laplace equation. Such a treatment allows one to prescribe freely the level of divergence inside the body by satisfying a modified divergence condition expressed as

$$\nabla \cdot \mathbf{u}^{k+1} = \nabla \cdot (\varepsilon {\mathbf{u}_0}^{k+1}). \tag{12}$$

The creation of an internal motion given by the target velocity introduces a mass source/sink inside the body. This artificial flow based on a "mirror velocity strategy" is useful for the regularity of the solution when the boundary of the solid body does not coincide with the Cartesian mesh.[51]

5. Validations of the Numerical Method and Comparisons with Experimental Results

The simulations presented here correspond to a fractal cross grid with three fractal iterations — that of Fig. 3(a) of Ref. 15.

5.1. *Configuration of the flow*

Only one multiscale grid will be considered here and it is from the family of fractal cross grids (Fig. 1, left). This grid is completely characterised by

- The number of fractal iterations N ($N = 3$ in Fig. 1, left);
- The bar lengths $L_j = R_L^j L_0$ and the thicknesses $t_j = R_t^j t_0$ (in the plane of the grid, normal to the mean flow) at iteration j, $j = 0, \ldots, N-1$ (all these bars have the same 5 mm thickness in the direction of the mean flow);
- The number (B^j) of patterns at iteration j.

Note that $B = 4$, $N = 3$, $R_L = 1/2$ and $R_t = 0.55$ for the cross grid considered here, which corresponds to one of the fractal cross grids used by Hurst and Vassilicos.[15] By definition, $L_0 = L_{\max}$, $L_{N-1} = L_{\min}$, $t_0 = t_{\max}$ and $t_{N-1} = t_{\min}$, and the grid in question has $t_{\max} = 62$ mm, $t_{\min} = 18.78$ mm and $L_{\max} = T = 0.91$ m. Our simulations aim at reproducing the same geometry. The blockage ratio σ of this grid is the ratio of their total area to the area T^2 of the tunnel's cross section ($T = 0.91$ m) and is equal to 40%. It is also of interest to define the thickness ratio

Table 1. Numerical parameters of the two DNSs.

DNS	$\mathrm{Re}_{t_{\min}}$	Δt	(n_x, n_y, n_z)	CORES
DNS_1	300	$0.0075 t_{\min}/U_\infty$	$(769, 256, 256)$	128
DNS_2	300	$0.0075 t_{\min}/U_\infty$	$(1537, 512, 512)$	256

$t_r = t_{\max}/t_{\min} = 3.3$. Unlike classical grids, fractal grids do not have a well-defined mesh size. Hurst and Vassilicos[15] introduced an effective mesh size for fractal grids defined as

$$M_{\mathrm{eff}} = \frac{4T^2}{P}\sqrt{1-\sigma}\,,$$

where P is the fractal perimeter's length of the grid. Note that the fractality of the grids influences M_{eff} via their perimeter P, which can be extremely long in spite of being constrained to fit within the area T^2. For this particular grid, $M_{\mathrm{eff}} = 114$ mm.

As this is the first time that a realistic DNS is conducted of a multiscale-generated turbulent flow which can be closely compared to an existing experiment, it is important to validate carefully the numerical method and also determine the numerical constraints of the simulations (Reynolds number, number of mesh nodes, size of the computational domain, and memory). In fact, due to the multiscale nature of the flow, these simulations require state-of-the art top-end parallel computing and therefore the number of mesh nodes is of crucial importance. Note that these simulations could not have been performed with second-order schemes. Indeed, preliminary studies (not presented here) have shown that a simulation with second-order schemes requires 3.5 more mesh nodes in each spatial direction for the statistical results to be the same as those of a simulation with sixth-order schemes.

One of the imperatives of this preliminary numerical study is to be as close as possible to the experimental set-up of Hurst and Vassilicos,[15] who conducted hot wire measurements in a horizontal wind tunnel for a flow of mean free stream $U_\infty = 12$ m/s. The parameters of the targeted grid correspond to the experimental ones. The numerical parameters (computational size domain, time step, Reynolds number, mesh nodes, etc.) are determined to be as close to the experimental conditions as possible, except for the Reynolds number $\mathrm{Re}_{t_{\min}} = \frac{U_\infty t_{\min}}{\nu}$, which must be reduced from 14 400 to 300 despite the use of high resolution DNS (up to 400 million mesh nodes). Consequently, only qualitative agreement with experiments can be expected. In order to validate the number of mesh nodes needed to discretise the smallest thickness $t_{\min}$ and to have good agreement with the experimental results, two simulations have been performed where the governing equation has been solved in a computational domain $(L_x,\ L_y,\ L_z) = (153.6t_{\min}, 51.t_{\min}2, 51.2t_{\min})$ (see Fig. 2 for a schematic view of the flow configuration). The resolution, time step and number of computational cores of each simulation are given in Table 1.

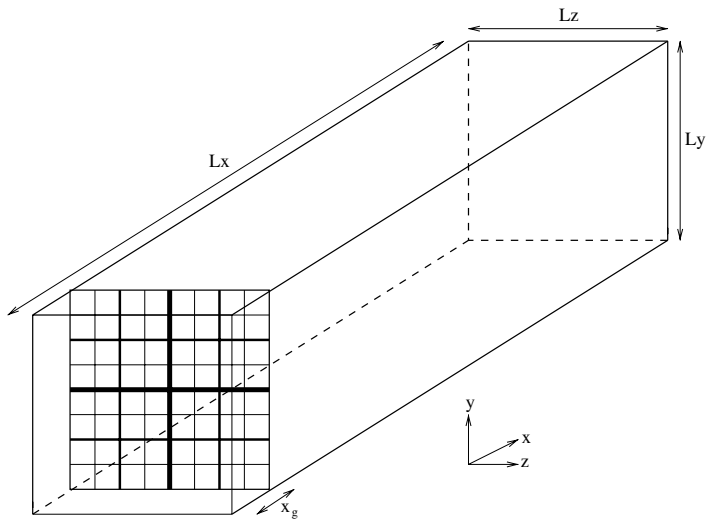

Fig. 2. Schematic view of the flow configuration with a fractal cross grid.

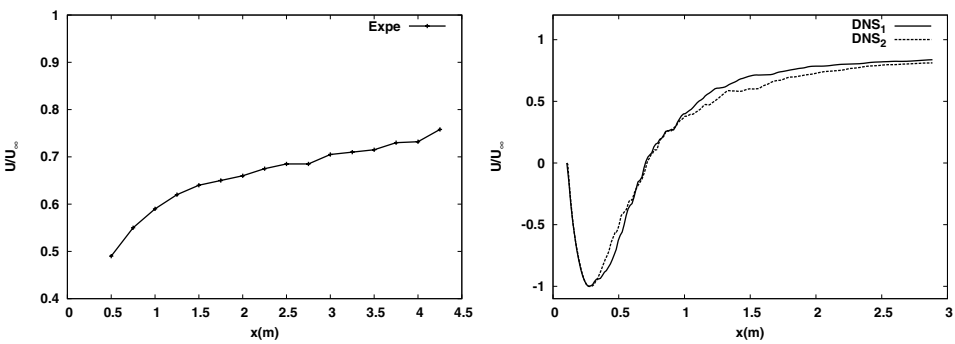

Fig. 3. Streamwise evolution of U/U_∞ on the centreline for the experimental data (left) and the numerical data (right).

5.2. *DNS results*

We have run our code twice with identical sets of parameters except for the number of mesh points (see Table 1). We refer to the run with the lower spatial resolution as DNS_1 and to the run with the higher spatial resolution as DNS_2. One of the objects of this exercise is to establish the resolution necessary for obtaining turbulence statistics which match, at least qualitatively, those obtained by Hurst and Vassilicos[15] in their wind tunnel experiments.

It is very difficult to obtain well-converged statistics from our DNS, as it is meaningless to average over space because of the inhomogeneity in the production region upstream from the fractal grid. Statistics are therefore obtained by averaging

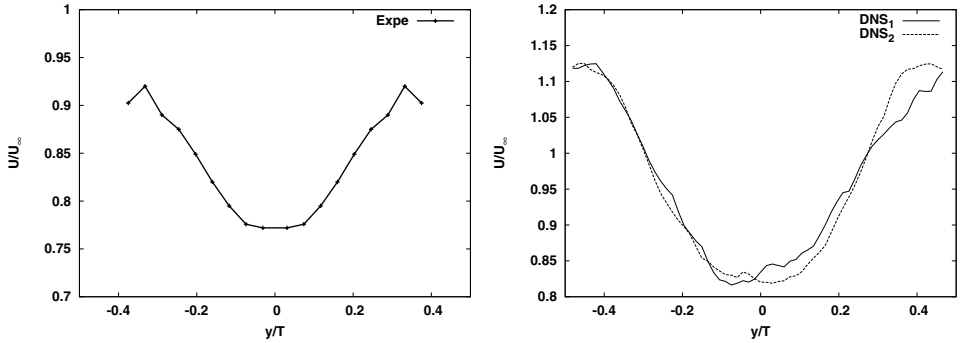

Fig. 4. Mean flow profile: U/U_∞ in the y direction, at $x = 2.24\,\mathrm{m}$ and $x = 4.25\,\mathrm{m}$ for the experimental data (left) and the numerical data (right).

over time at given spatial locations, providing mean flow and turbulence profiles as functions of streamwise distance x and lateral coordinate y.

For both DNS_1 and DNS_2 we had to establish the time in the simulation when statistics could start being collected, as well as the duration of this collection. After some experimentation we chose this starting time to be 200 $t_{\min}/U_\infty$ and the averaging time (collection duration) to be 400 $t_{\min}/U_\infty$. The flow downstream from the fractal grid was fully turbulent during this time period. Our choice of transient time, 200 $t_{\min}/U_\infty$ was shored up by comparing second-order moments obtained by averaging over the same duration, 400 $t_{\min}/U_\infty$, but with different starting times: 180, 200, 220 and 240 $t_{\min}/U_\infty$. There was less than a 5% difference in these statistics with a starting time of 220 $t_{\min}/U_\infty$ rather than 200 $t_{\min}/U_\infty$. Our choice of averaging time was also given some support by trying different averaging times (300, 350, 400, 450 and 500 $t_{\min}/U_\infty$) following the same starting time, 200 $t_{\min}/U_\infty$, in all cases. We found a difference of less than 5% between the 400 and 450 $t_{\min}/U_\infty$ cases.

In their experimental measurements, Hurst and Vassilicos[15] observed that fractal cross grids generate non-zero values of $\frac{\partial U}{\partial x}$ on the tunnel's centreline whereas classical grids do not (U is the local mean flow velocity in the streamwise direction). This particular behaviour is also observed in our DNSs which agree qualitatively with the wind tunnel experiments at the large-enough streamwise distances where the hot wire measurements were taken (see Fig. 3). It must be stressed again that the Reynolds number in the experiment is much higher than in our simulations and therefore no exact quantitative agreement should be expected. Our simulations reveal a significantly large recirculation region with negative values of U near the grid (see Fig. 3). This recirculation region was clearly identified in a movie of the numerically simulated centreline streamwise velocity near the grid and represents a clear prediction for future experimental measurements to be made closer to the grid and at lower Reynolds numbers. As mentioned by Hurst and Vassilicos,[15] these gradients of U along x must be offset by lateral gradients of U in the y, z

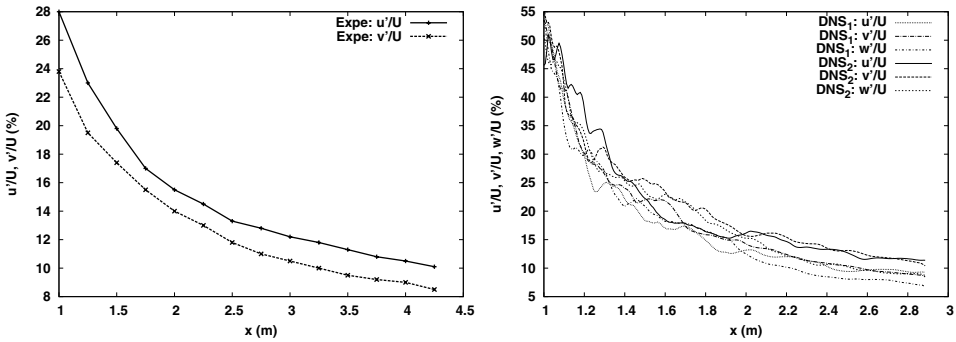

Fig. 5. Turbulence decay on the centreline for experimental data (left) and numerical data (right).

plane. Figure 4 shows the mean flow profile inhomogeneity in the y direction and establishes that it is qualitatively very similar in our DNS and in the wind tunnel measurements, even though they are taken at different distances from the grid and different Reynolds numbers.

In Fig. 5 we plot the centreline streamwise decay of turbulence intensities. Our numerical simulations confirm the high turbulence intensities returned by fractal turbulence actuation. Whilst the streamwise decay is also qualitatively similar between experiment and simulation, the actual turbulence intensity values are very different close to the grid (by a factor of 2 at $x = 1\,\mathrm{m}$). Nevertheless, at distances $x = 2\,\mathrm{m}$ and beyond the turbulence intensities are quantitatively similar. The Reynolds numbers are significantly different between simulation and experiment and it may well be possible that the recirculation bubble observed in our simulation is a low Reynolds number feature which diminishes in size as the Reynolds number increases so that 55% turbulence intensities might be observed at higher Reynolds numbers only at that diminished distance from the grid where the recirculation bubble might still exist, if it exists at all. These are relevant and interesting questions raised by our DNS for experimental wind tunnel measurements which might not have been raised otherwise.

In Fig. 6 we compare the large-scale turbulence anisotropy obtained experimentally and from our DNS. Whilst our DNS statistics are clearly not as well converged as the wind tunnel statistics, one can make out a general agreement. For example, the two symmetric peak anisotropies are located roughly at the same values of y and are close to 1.5 in both the DNS and the wind tunnel. This comparison is made at a value of x large enough for one to expect, perhaps, minimal Reynolds number effect on the turbulence intensity ratios which measure turbulence anisotropy.

Finally, we point out that all the DNS_1 and all the DNS_2 statistics presented here are in good agreement with each other. Hence, the spatial mesh resolution employed is good enough for these statistics.

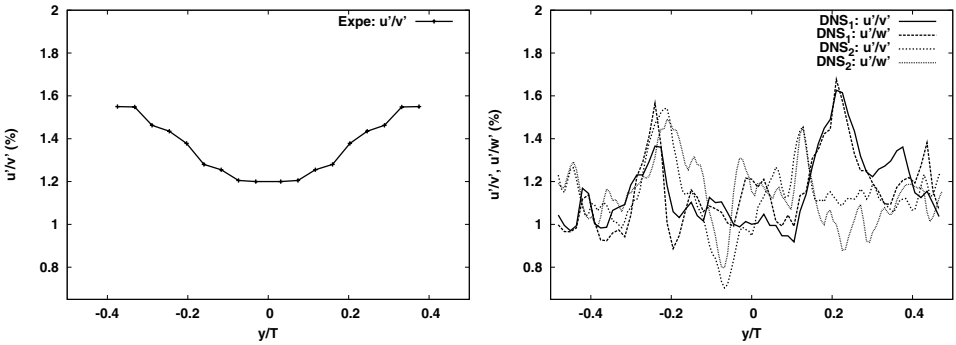

Fig. 6. Turbulence anisotropy profiles. Left: Experimental data at $x = 4.25$ m. Right: Numerical data at $x = 2.24$ m.

6. Conclusions

The general fields of non-linear physics and engineering of multiscale objects, in particular non-linear fluid mechanics of multiscale flow actuation, are extremely promising emerging fields of investigation. This paper establishes IBM-based DNS as a valid tool for the study of multiscale-generated turbulence. Current terascale and future petascale high-performance computing capabilities make the use of this tool viable for the investigation of this new field. It should be used in conjunction with novel developments in turbulence measurement techniques, such as state-of-the art stereoscopic and high-speed particle image velocimetry (SPIV),[55] particle-tracking velocimetry and accelerometry (PTVA),[56] and multi-hot/cold wire anenometry (MHCWA).[57]

Acknowledgments

We acknowledge the EPSRC UK Turbulence consortium and EPSRC grant EP/F051468 for the CPU time made available to us on HECToR, without which this paper would not have been possible. We are grateful to Roderick Johnstone for help with the parallel version of Incompact3d. We also thank Eric Lamballais for very useful discussions and acknowledge the support from EPSRC research grant EP/E00847X.

References

1. C. Caratheodory, Nachrichten der K. Gesellshaft der Wissenschaften zu Gottingen, *Mathematisch-Physikalische Klasse* (1914) 404–426. Also in *Caratheodory, Gesammelte Mathematische Schriften* (Beck, Munich, 1954).
2. F. Hausdorff, Dimension und auβeres Maβ, *Math. Ann.* **79** (1918) 157–179.
3. K. J. Falconer, *Fractal Geometry: Mathematical Foundations and Applications* (John Wiley & Sons, Chichester, 1990).
4. B. Mandelbrot, *Fractals, Form, Chance and Dimensions* (W. H. Freeman, San Francisco, 1977).

5. B. Mandelbrot, *The Fractal Geometry of Nature* (W. H. Freeman, San Francisco, 1982).
6. L. P. Kadanoff, Fractals: Where's the physics?, *Phys. Today* **36** (1986) 6–7.
7. M. V. Berry, Falling fractal flakes, *Physica D* **38** (1989) 29–31.
8. B. Sapoval and Th. Gordon, Vibrations of strongly irregular or fractal resonators, *Phys. Rev. E* **47** (1993) 3013–3024.
9. M. Lapidus *et al.*, Snowflake harmonics and computer graphics: numerical computation of spectra on fractal domains, *Int. J. Bifur. Chaos Appl. Sci. Eng.* **6** (1996) 1185–1210.
10. J. Fleckinger, M. Levitin and D. Vassiliev, Heat equation on the triadic von Koch snowflake: Asymptotic and numerical analysis, *Proc. London Math. Soc.* **71** (1995) 372–396.
11. M. van den Berg, Heat content and Brownian motion for some regions with a fractal boundary, *Prob. Theory Related Fields* **100** (1994) 439–456.
12. W. C. Kim and R. Mauborgne, Knowing a winning business idea when you see one, *Harvard Bus. Rev.* (Sep.–Oct. 2000).
13. A. Adrover and M. Giona, Hydrodynamic properties of fractals: Application of the lattice Boltzmann equation to transverse flow past an array of fractal objects, *Int. J. Multiphase Flow* **23** (1997) 25–35.
14. S. W. Coleman and J. C. Vassilicos, Tortuosity of saturated and unsaturated porous fractal materials, *Phys. Rev. Lett.* **100** (2007) 035504.
15. D. Hurst and J. C. Vassilicos, Scalings and decay of fractal-generated turbulence, *Phys. Fluids* **19** (2007) 035103.
16. R. E. Seoud and J. C. Vassilicos, Dissipation and decay of fractal-generated turbulence, *Phys. Fluids* **19** (2007) 105108.
17. D. Queiros-Conde and J. C. Vassilicos, Turbulent wakes of 3-D fractal grids, *Intermittency in Turbulent Flows and Other Dynamical Systems*, eds. J. C. Vassilicos (Cambridge University Press, 2001).
18. P. G. de Gennes, *Introduction to Polymer Physics* (Cambridge University Press, 1990).
19. P. G. de Gennes, *Scaling Concepts in Polymer Physics* (Cornell University Press, Ithaca, 1979).
20. R. H. Shaw and E. G. Patton, Canopy element influences on resolved- and subgrid-scale energy within a large-eddy simulation, *Agr. Forest Meteorol.* **115** (2003) 5–17.
21. M. P. Coutts and J. Grace, *Wind and Trees* (Cambridge University Press, 1995).
22. J. A. Kaadrop, E. A. Koopman, P. M. A. Sloot, R. P. M. Bak, M. J. A. Vermeij and L. E. H. Lampmann, *Philos. Trans. R. Soc. Lond. B* **358** (2003) 1551–1557.
23. C. van Ertbruggen, C. Hirsch and M. Paiva, Anatomically based three-dimensional model of airways to simulate flow and particle transport using computational fluid dynamics, *J. Appl. Physiol.* **98** (2005) 970–980.
24. C. Coffey, G. Hunt, R. E. Seoud and J. C. Vassilicos, Proof of concept report for the attention of Imperial Innovations (2007). http://www3.imperial.ac.uk/tmfc/people/j.c.vassilicos/recentpublications
25. R. E. Seoud and J. C. Vassilicos, Passive multiscale flow control by fractal grids, *IUTAM Symp. Flow Control and MEMS*, eds. J. F. Morrison, D. M. Birch and P. Lavoie (2008).
26. S. Ferrari, P. Kewcharoenwong, L. Rossi and J. C. Vassilicos, Multiscale flow control for efficient mixing: Laboratory generation of unsteady multiscale flows controlled by multiscale electromagnetic forcing, *IUTAM Symp. Flow Control and MEMS*, eds. J. F. Morrison, D. M. Birch and P. Lavoie (2008).

27. K. Nagata, H. Suzuki, Y. Sakai and T. Kubo, Direct numerical simulations of fractal grid-generated turbulence, APS, Division of Fluid Mechanics, Salt Lake City, Utah, 18–20 November, 2007.
28. U. Frisch, *Turbulence*: *The Legacy of A. N. Kolmogorov* (Cambridge University Press, 1995).
29. S. B. Pope, *Turbulent Flows* (Cambridge University Press, 2000).
30. S. Chester, C. Meneveau and M. B. Parlannge, Modelling turbulent flow over fractal trees with renormalized numerical simulation, *J. Comput. Phys.* **225** (2007) 427–448.
31. R. E. Seoud and J. C. Vassilicos, Fully developed turbulence with diminishing mean vortex stretching and reduced intermittency. Submitted (2008).
32. G. I. Taylor, Statistical theory of turbulence, *Proc. R. Soc. London A* **151** (1935) 421–478.
33. A. Tsinober, *An Informal Introduction to Turbulence* (Kluwer, Dordrecht/Boston/London, 2001).
34. S. K. Lele, Compact finite difference schemes with spectral-like resolution, *J. Comput. Phys.* **103** (1992) 16–42.
35. C. S. Peskin, Flow patterns around heart valves: A numerical method, *J. Comput. Phys.* **10** (1972) 252–271.
36. C. S. Peskin, The immersed boundary method, *Acta Numer.* **11** (2002) 479–517.
37. H. S. Udaykumar, W. Shyy and M. M. Rao, Elafint: A mixed Eulerian–Lagrangian for fluid flows with complex and moving boundaries, *Int. J. Numer. Methods Fluids* **22** (1996) 691–705.
38. T. Ye, R. Mittal, H. S. Udaykumar and W. Shyy, An accurate Cartesian grid method for viscous incompressible flows with compex immersed boundaries, *J. Comput. Phys.* **156** (1999) 209–240.
39. E. A. Fadlum, R. Verzicco, P. Orlandi and J. Mohd-Yusof, Combined immersed boundary finite-difference methods for three-dimensional complex flow simulations, *J. Comput. Phys.* **161** (2000) 35–60.
40. R. Mittal and G. Iaccarino, Immersed boundary methods, *Ann. Rev. Fluid Mech.* **37** (2005) 239–261.
41. D. Goldstein, R. Handler and L. Sirovich, Modeling a no-slip boundary condition with an external force field, *J. Comput. Phys.* **105** (1993) 354–366.
42. E. Arquis and J. P. Caltagirone, Sur les conditions hydrodynamiques au voisinage d'une interface milieu fluide-milieu poreux: Application la convection naturelle, *CRAS, Série II* **299** (1984) 1–4.
43. A. J. Chorin, Numerical solution of the Navier–Stokes equations, *Math. Comput.* **22** (1968) 745–762.
44. R. Temam, Sur l'approximation de la solution des equations de Navier–Stokes par la methode des pas fractionnaires (I), *Arch. Rat. Mech. Anal.* **32** (1969) 135–153.
45. J. Kim and P. Moin, Application of a fractional-step method to incompressible Navier–Stokes equations, *J. Comput. Phys.* **59** (1985) 308–323.
46. J. B. Perot, An analysis of the fractional step method, *J. Comput. Phys.* **108** (1993) 51–58.
47. W. Chang, F. Giraldo and B. Perot, Analysis of an exact fractional step method, *J. Comput. Phys.* **180** (2002) 183–199.
48. A. B. Cain, J. H. Ferziger and W. C. Reynolds, Discrete orthogonal function expansions for non-uniform grids using the fast Fourier transform, *J. Comput. Phys.* **56** (1984) 272.
49. S. Laizet and E. Lamballais, Compact schemes for the DNS of incompressible flows: In what context is the quasi-spectral accuracy really useful?, *Proc. IV Escola de Primavera de Transiçao e Turbulência*, Porto Alegre, Brazil (2004).

50. S. Laizet and E. Lamballais, High-order compact schemes for incompressible flows: A simple and efficient method with the quasi-spectral accuracy. Submitted to *J. Comput. Phys.* (2008).
51. P. Parnaudeau, E. Lamballais and J. H. Silvestrini, Combination of the immersed boundary method with compact schemes for DNS of flows in complex geometry, *Proc. DLES-5*, Munich (2003).
52. J. H. Silvestrini and E. Lamballais, Direct numerical simulation of oblique vortex shedding from a cylinder in shear flow, *Int. J. Heat Fluid Flow* **25** (2004) 461–470.
53. P. Parnaudeau, J. Carlier, D. Heitz and E. Lamballais, Experimental and numerical studies of the flow over a circular cylinder at Reynolds number 3900. Submitted to *Phys. Fluids* (2006).
54. P. Parnaudeau, D. Heitz, E. Lamballais and J. H. Silvestrini, Vortex shedding behind cylinders with spanwise linear nonuniformity, *J. Turbulence* **8** (2007) 1–13.
55. B. Ganapathisubramani, K. Lakshminarasimhan and N. T. Clemens, Investigation of three-dimensional structure of fine scales in a turbulent jet by using cinematographic stereoscopic particle image velocimetry, *J. Fluid Mech.* **598** (2008) 141–175.
56. S. Ferrari and L. Rossi, Particle tracking velocimetry and accelerometry (PTVA) measurements applied to quasi-two-dimensional multiscale flows, *Exp. Fluids* **44** (2008) 873–886.
57. A. Tsinober, E. Kit and T. Dracos, Experimental investigation of the field of velocity gradients in turbulent flows, *J. Fluid Mech.* **242** (2008) 169–192.
58. K. Nagata, H. Suzuki, Y. Sakai, T. Hayase and T. Kubo, Direct numerical simulation of turbulent mixing in grid-generated turbulence, *Phys. Scripta* (2008), in press.